Spatiotemporal regulation of chemical reactions by active cytoskeletal remodeling

Abhishek Chaudhuri[a,b,c,1], Bhaswati Bhattacharya[d,1], Kripa Gowrishankar[a,e], Satyajit Mayor[e], and Madan Rao[a,e,2]

[a]Raman Research Institute, C. V. Raman Avenue, Bangalore 560080, India; [b]Department of Biomedical Science, University of Sheffield, Sheffield S10 2TN, United Kingdom; [c]The Rudolf Peierls Centre for Theoretical Physics, University of Oxford, Oxford OX1 3NP, United Kingdom; [d]Theoretical Studies Unit, Jawaharlal Nehru Centre for Advanced Scientific Research, Jakkur Campus, Bangalore 560080, India; and [e]National Centre for Biological Sciences (TIFR), Bellary Road, Bangalore 560065, India

Edited* by Ronald D. Vale, University of California, San Francisco, CA, and approved July 25, 2011 (received for review January 12, 2011)

Efficient and reproducible construction of signaling and sorting complexes, both on the surface and within the living cell, is contingent on local regulation of biochemical reactions by the cellular milieu. We propose that in many cases this spatiotemporal regulation can be mediated by interaction with components of the dynamic cytoskeleton. We show how the interplay between active contractility and remodeling of the cytoskeleton can result in transient focusing of passive molecules to form clusters, leading to a dramatic increase in the reaction efficiency and output levels. The dynamic cytoskeletal elements that drive focusing behave as *quasienzymes* catalyzing the chemical reaction. These ideas are directly applicable to the cortical actin-dependent clustering of cell surface proteins such as lipid-tethered GPI-anchored proteins, Ras proteins, as well as many proteins that have domains that confer the ability to interact with the actin cytoskeleton. In general such cytoskeletal driven clustering of proteins could be a cellular mechanism to spatiotemporally regulate and amplify local chemical reaction rates in a variety of contexts such as signaling, transcription, sorting, and endocytosis.

active hydrodynamics | signal transduction

The living cell constructs and dissipates signaling and sorting complexes at particular locations in space and at precise times. This requires the regulated (de)activation, (dis)assembly, and possibly spatial localization of specific molecular components and regulatory elements and must occur with high efficiency, reproducibility, and fidelity in a noisy and overcrowded cellular environment. It is highly unlikely that the spatiotemporal control of such multimolecular processes in the cell should depend on thermal diffusive processes alone.

In this paper, we propose that the active local remodeling of the cytoskeleton that pervades the cell—from the cell cortex, to the cytoplasm, to within the nucleus—can spatiotemporally regulate biochemical reactions leading to significantly higher efficiency. We show how such constitutively *active* processes can drive a unique molecular complexation, whose robustness can be altered by tuning the local remodeling dynamics of the cytoskeleton or by modulating the affinity of the reactants or their regulators to the components of the cytsokeleton. Chemical reactions or signaling processes contingent on this complexation, such as those involving allostery (1, 2), cooperative binding (3) etc., will be strongly amplified by such active mechanisms, especially when the concentration of reactants is low. This is by no means the only agency for spatiotemporal regulation and amplification—other mechanisms may act independent of or in conjunction with the one proposed here.

Examples where these active mechanisms might be at work are in the localization and activation of specific Rab-GTPases on distinct endosomes in precise regions of the cytoplasm (4), and in the localization and targeted movement of transcription factories in the cell nucleus (5).

In the context of the two-dimensional cell surface, which will largely be the focus of this paper, cell surface receptors, especially lipid-tethered signaling receptors, such as the outer leaflet CD-59, a GPI-anchored protein (GPI-AP) (6) and the inner leaflet Ras family of GTPases (7–9) form transient signaling platforms, which are highly efficient in recruiting downstream components, such as Src-family kinases. There is growing evidence that the formation of transient signaling platforms and the recruitment of the downstream effectors involves a coupling to the dynamic cortical actin (CA) (8, 10).

This coupling between lipid-tethered proteins and the active remodeling dynamics of CA has been made sharper by recent experiments using a variety of FRET (10, 11) and high-resolution imaging (8, 12), which show that these molecules form nanoclusters harboring multiple species of the protein (11); the dynamics of formation and breakup is controlled by the dynamics of remodeling of the adjoining CA. The nanoclusters, when they form, are effectively immobilized by the local cortical actin (10).

In this paper we propose that the remodeling and contractile dynamics of cytoskeletal filaments can transiently focus the organization of passive molecules (i.e., molecules that transiently bind and unbind to the cytoskeletal filaments) to form dynamic clusters (13). This active clustering of passive molecules can serve as reaction platforms, leading to a significant enhancement of chemical reaction rates, when the active Peclet number, defined as the ratio of the advection to diffusion rates, is high. Optimal efficiency occurs when a certain *active resonance* condition is met : when the time scales of active advection along cytoskeletal filaments are comparable to the active remodeling time. In such situations the active cytoskeletal elements behave as a quasienzyme catalyzing the chemical reactions.

Our proposal, although theoretical, is grounded in the well-accepted formalism of *active hydrodynamics* for the coupled dynamics of cytoskeletal filaments and motors (14–19) which has been successfully applied in several cellular contexts such as wound healing and the onset of cytokinesis (20) and cell polarization (21).

Model

Molecular Clustering Induced by Cytoskeletal Remodeling. The active remodeling and contractile dynamics of cyto(nucleo)-skeletal filaments in two or three dimensions (2D or 3D), can be theoretically studied using a set of coarse-grained equations for the local filament concentration c and orientation field, which for polar (apolar) filaments, is represented by a vector, $\mathbf{n}$ (tensor, Q_{ij}). Activity, due to bound motors and/or treadmilling, induces

Author contributions: A.C., B.B., K.G., S.M., and M.R. designed research; A.C., B.B., K.G., S.M., and M.R. performed research; A.C., B.B., K.G., S.M., and M.R. analyzed data; and A.C., B.B., K.G., S.M., and M.R. wrote the paper.

The authors declare no conflict of interest.

*This Direct Submission article had a prearranged editor.

[1]A.C. and B.B. contributed equally to this work.

[2]To whom correspondence should be addressed. E-mail: rao.madan@gmail.com.

This article contains supporting information online at www.pnas.org/lookup/suppl/doi:10.1073/pnas.1100007108/-/DCSupplemental.

contractile stresses $\sigma^{(a)} \propto c\mathbf{nn}$ (polar) or cQ (apolar), and currents $\mathbf{J} \propto c\mathbf{n}$ (polar) or $c\nabla \cdot Q$ (apolar) in the fluid medium (14–16).

For simplicity, we display only the dynamical equations for active polar filaments in 2D and 3D. Numerical analysis of the equations is restricted to the case of 2D, directly relevant to the dynamics of cortical actin on the cell surface; however, our qualitative findings carry through in 3D. We assume that the cytoskeletal mesh provides a momentum sink because of frictional dissipation and so ignore the hydrodynamic velocity.

Activity originating from filament-motor contractility (actomyosin contractility in the case of CA) and possibly treadmilling, induce relative motion of the polar filaments with respect to the embedding medium, along the direction of polarization. Over time scales smaller than filament turnover, the local filament concentration c is a conserved variable and obeys a continuity equation,

$$\partial_t c = -\nabla \cdot \mathbf{J} \qquad [1]$$

where $\mathbf{J}$ is the current given by the sum of an active advection (with a speed v) along the polar filaments and filament diffusion (D_f is the trace of the filament diffusion matrix), $\mathbf{J} = vc\mathbf{n} - D_f \nabla c$.

The coarse-grained dynamics of filament orientation $\mathbf{n}$ is given by a generalization of the equations of liquid crystal hydrodynamics to include activity (14–19),

$$\partial_t \mathbf{n} + \underbrace{\lambda(\mathbf{n}\cdot\nabla)\mathbf{n}}_{\text{active advection}} = K_1\nabla^2\mathbf{n} + K_2\nabla(\nabla\cdot\mathbf{n}) \underbrace{+\zeta\nabla c + \alpha\mathbf{n} - \beta|\mathbf{n}|^2\mathbf{n}}_{\text{actomyosin contractility}} + \ldots + \mathbf{f}_n, \qquad [2]$$

where we have highlighted the active contributions coming from actomyosin contractile forces; the "…" contain terms higher order in the fields and gradients (13). The *active* noise $\mathbf{f}_n$, representing the ambient stochasticity in the medium due to binding/unbinding of motors, is spatiotemporally uncorrelated, with a variance proportional to cT_a, an activity temperature. The "Frank constants" K_1, K_2 describe the scale over which the polar filaments undergo splay and bend distortions. The coefficients $\alpha,\beta > 0$ ensure that the magnitude of $\mathbf{n}$ is nonzero. Finally, for contractile actomyosin, $\zeta v > 0$.

These sets of equations can be solved numerically within a domain with periodic boundary conditions to obtain a phase diagram of steady states (13). The steady state configurations in 2D consist of a finite density of *localized, inward-pointing* "asters," which constantly remodel (break up and reform), as a consequence of the active temperature T_a. At low T_a, aster remodeling is negligible; the size of the localized asters is set by a competition between active advection and filament diffusion, D_f/v, whereas the scale between asters, and hence the aster density ρ_a, is set by K_1/ζ. At high T_a, remodeling is significant and the aster length scales are sensitive to T_a. The remodeling times (lifetimes) show an exponential distribution (13) with a mean τ_a that goes as $\exp(1/T_a)$ over a wide range of parameters.

Before we move on, we make two observations: (*i*) Even if the filaments are apolar, the steady state in 2D would still consist of asters and (*ii*) in 3D, the corresponding localized and transient defect configurations are the active version of the inward-pointing *hedgehogs*, a 3D generalization of asters (see ref. 22 for a description of hedgehog configurations in equilibrium spin systems).

We now study the influence of this dynamic patterning of cytoskeletal filaments on the dynamics of *passive* molecules, defined as molecules that transiently bind to the active filaments, but do not influence the organization of the cytoskeleton. In general, even without the aid of a detailed model, one would expect that a gradient in active stresses would give rise to a passive particle current, proportional to $\nabla \cdot \sigma^{(a)}$, true for both polar and apolar filaments in two and three dimensions. This would lead to a clustering at the sites of asters (hedgehogs), which would be transient owing to the finite lifetime of the aster (hedgehog).

For specificity, we focus on the dynamics of passive cell surface molecules, such as GPI-AP or a transmembrane protein, whose binding with the CA could be either a result of a direct interaction or an indirect interaction mediated by other membrane molecules (23, 24). In either case, the passive molecule once bound will be advected along the active polar filament, while undergoing thermal diffusion in the unbound state—this suggests the following stochastic dynamics for the instantaneous position of the passive molecule:

$$\mathbf{x}(t) = \mathbf{x}(0) + \int_0^t \mathbf{v}(t')dt'$$
$$\mathbf{v}(t) = \phi(t)vc(\mathbf{x}(t),t)\mathbf{n}(\mathbf{x}(t),t) + (1-\phi(t))\mathbf{f}(t), \qquad [3]$$

where ϕ is a two-state random variable and takes values 1 (bound) and 0 (unbound). We characterize this telegraphic noise (25) by stochastic switching rates between these states k^{on} and k^{off}, or the *mean duty ratio*, $K \equiv \langle\phi\rangle = \frac{k^{\text{on}}}{k^{\text{on}}+k^{\text{off}}}$ and *mean switching time*, $t_{\text{sw}} = \frac{2}{k^{\text{on}}+k^{\text{off}}}$. When unbound, the velocity of the passive molecule is given by a thermal white noise $\mathbf{f}(t)$ with zero mean and variance proportional to D, the diffusion coefficient of the passive molecule.

If the time scales for particle advection are much shorter than the remodeling time τ_a of the actin asters, then passive molecules with a high duty ratio K will be driven to the cores of the inward-pointing asters (hedgehogs) by the dynamics Eq. **3**. This is the origin of the active actin based clustering of cell surface molecules, observed and described in refs. 10 and 13. As the aster remodels, the cluster of passive particle fragments only to reform elsewhere. Because the active noise reduces the mean size R of the aster (13), the time taken for a bound particle to advect over the scale of the aster τ_v reduces with T_a. Note that the aster size can vary from many tens of nanometers to microns, depending on the local cellular context.

Reaction Kinetics Affected by Active Stresses and Currents. Such transient, active localization of molecular clusters can have profound implications for signaling and chemical reactions, as we explore within simple biochemical reaction schemes. The influence of activity on chemical reaction kinetics could appear at various levels: (*i*) local active stress could induce conformation changes or modulation of molecular flexibility, which changes the Arrhenius factor, (*ii*) active enhancement of molecular transport (advection), focussing particle trajectories, localization, and breakup, which increase the attempt frequency of the chemical reaction, and (*iii*) cooperativity resulting in a high Hill coefficient for the chemical reaction. In this paper we discuss mainly the enhancement arising from active advection, localization, focusing, and breakup and leave an exploration of the more general issues to a later publication.

Because we are typically dealing with cell surface chemical reactions involving low concentration of reactants, we need to include the effects of stochasticity. This is conveniently done by generalizing Eq. **3** to include chemical reaction dynamics, which we solve using a Brownian dynamics simulation.

We point to a recent theoretical paper (26), which discusses the general idea of enhancement of chemical reaction rates by active transport along polar cytoskeletal filaments. However, these authors treat the cytoskeleton as a meshwork of long, *static* filaments that are *randomly oriented* in space. We will see that allowing the polar filaments to obey their natural dynamics in a living cell, Eq. **2**, opens up an additional dimension in the spatiotemporal regulation of chemical reactions occurring in such a milieu.

Brownian Dynamics Simulation of Chemical Reactions. We introduce N passive molecules (denoted by A) onto a 2D domain of area

$L \times L$ (representing, say, a patch of the plasma membrane); thus the areal density of molecules is N/L^2. To model the steady state configuration of CA within the domain, we decorate the domain with a *uniform distribution* of localized, inward-pointing asters of size R and density ρ_a. Strictly, we should have generated a spatial distribution according to Eq. **2**; however, we have checked that our results do not depend on the precise form of spatial distribution. In between asters, the filaments are oriented randomly with a uniform distribution between $[0,2\pi]$. The asters are modeled by polar filaments that point radially inward and terminate in a core of size r_c (Fig. 1). The concentration of filaments within the aster is taken to be a constant c_0 (13); as we see below, our qualitative results are independent of the form of the concentration profile. The CA asters remodel (break up and reform elsewhere) in a time taken from an exponential distribution with mean given by τ_a.

To model the stochastic dynamics of passive molecules (simulation details in *SI Text*), note that the filament concentration profile within the aster appears as an effective capture cross-section, $\Sigma \sim KR^2 c_0 \rho_a$, of passive particles; once bound to the filaments in the aster, the molecules are advected toward the core with a speed v. Because the filaments in between asters are randomly oriented, even the dynamics of *bound* molecules in this region is diffusive, with an active diffusion coefficient set by the orientational correlation between filaments. For simplicity, we combine the active and thermal diffusion together in a single effective diffusion coefficient D. We perform Brownian dynamics updates on the passive particle positions (27),

$$\mathbf{x}_{i+1} = \mathbf{x}_i + \mathbf{v}_i \Delta t \qquad \mathbf{v}_i = \begin{cases} v\hat{\mathbf{n}}(\mathbf{x}_i) & \text{if bound, } \phi_i = 1 \\ \mathbf{f}_i & \text{if unbound, } \phi_i = 0 \end{cases}, \qquad [4]$$

where the notation is the same as Eq. **3**. We work in dimensionless units, where length is measured in units of the smallest scale, the size of the passive molecule σ, and time is set by the diffusion time, $\tau_d = \sigma^2/D$, and $\triangle t = 0.1\tau_d$.

Having set up the *advection-diffusion* dynamics of the passive molecules A, we now apply it to chemical kinetics. In this paper, we consider simple generic reaction schemes of the kind displayed in Fig. 2 *A–D*, which can take place in two or three dimensions.

In general, these chemical reactions could be either irreversible or reversible, with forward rates k_f and backward rates k_b. Molecules engage in a chemical reaction when brought to within a reaction radius of each other, which we take to be r_c—thus the cores of aster become reaction zones (Fig. 1). In all cases we ask how fast and to what extent does the reaction proceed.

We list all time scales in units of τ_d: (*i*) τ_v, advection time; (*ii*) τ_a, aster remodeling time; (*iii*) k_{on}^{-1}, k_{off}^{-1}, the binding/unbinding times, or alternatively, the duty ratio K and the switching time, t_{sw}; and (*iv*) k_f^{-1}, k_b^{-1}, forward/backward reaction times. The range of molecular diffusion coefficients $D = [0.01 - 1]\mu\text{m}^2/\text{s}$ (28); thus in units of $\tau_d = \sigma^2/D$, the range of $\tau_v = [0.1,10^4]$ and $\tau_a = [10,10^5]$.

Results

Second-Order Chemical Reactions: Cell Surface Signaling. Consider simple second-order chemical reactions, such as Fig. 2*A*, which describes a state change of the reactant A to its *activated* homologue, A^*, which could be allosterically enhanced. Alternatively, the activation could be modulated by the concentration of an effector molecule or enzyme B. In either case, the output A^* could result in a downstream signal.

The CA activity induced enhancement of chemical reactions is best studied when the reactions are *irreversible*, $k_b = 0$. As "control," we consider freely diffusing molecules A (and A^*) that do not interact with the CA, i.e., the duty ratio $K = 0$, and react irreversibly upon collision. Define $M(t) = N_{A^*}(t)/N$, the instantaneous fraction of the activated population A^*, from the dynamics we can compute the *mean activation time* τ and the *saturation output* M_∞ (here $M_\infty = 1$)—for free diffusion dynamics, $\tau \sim \tau_d L^2/N$. We plot the gain in activation rate due to CA activity, $G_\tau \equiv \tau_{\text{diff}}/\tau_{\text{act}}$, where τ_{diff} and τ_{act} are the mean activation times for free diffusion and active dynamics, respectively, versus various dynamical parameters (Fig. 3), for fixed aster density ρ_a and size R.

The relative contribution of active advection to the chemical reaction can be parametrized by a dimensionless *active Peclet number*, $P_e = KR\tau_d/\tau_v\sigma = KvR/D$ (29), the ratio of the rates of advection versus diffusion *over the size of the aster*. When $P_e \gg 1$, the chemical kinetics should be dominated by active advection. This is indeed what we observe in our simulations —keeping all other parameters fixed, we observe a sharp transition at $P_e \approx 10$ to a dynamical regime where the activation rate shows significant gain, $G_\tau > 1$ (Fig. 3*A*). We find that typically G_τ increases monotonically with K, and asymptotes to $G_\tau(K \to 1) \propto \tau_v^{-1}$ in contrast to ref. 26, and is a direct consequence of the dynamical steady states of the CA actin arising from Eqs. **1** and **2**.

On the other hand, the behavior of G_τ with the active remodeling time τ_a shows a nonmonotonic behavior. For values of τ_v corresponding to enhanced gain, $G_\tau(\tau_a \to 0) \sim 1 + G_1(\tau_v)\tau_a + \ldots$. The gain reaches a maximum, which can be very large for small τ_v (Fig. 3*B*), and asymptotes to $G_\tau(\tau_a \to \infty) \sim G_\infty + G_{-1}\exp(-\alpha(\tau_v)\tau_a) + \ldots$, where G_∞ is independent of τ_v. The maximum gain occurs when the $\tau_v = K\sigma\tau_a/R$ and represents a condition of *active resonance*; smaller asters need to be more frequently remodeled to meet this resonance. This is the active analogue of the well-known phenomenon of stochastic resonance

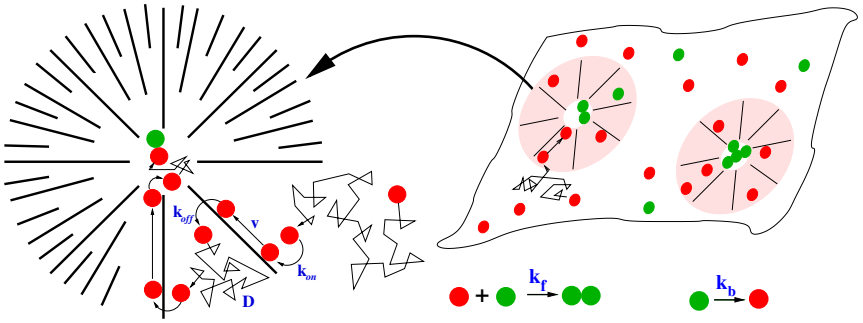

Fig. 1. Steady state configurations of active polar filaments in 2D (such as cortical actin at the cell surface) whose dynamics is given by Eqs. **1** and **2**, consist of a distribution of inward-pointing asters that stochastically remodel. The schematic shows the effect of having such asters on the kinetics of chemical reactions involving a state change from A (red) to A^* (green). The reactants can bind and unbind to the CA with rates k_{on} and k_{off}, respectively. Unbound reactants diffuse on the cell membrane with effective diffusion coefficient D, whereas bound reactants are advected toward the aster core with velocity v (magnified schematic (*Left*). Typical reactions occur with a forward rate k_f and backward rate k_b. The output A^* results in a downstream signal. Note that the essential feature of the active cytoskeletal dynamics that we exploit is the ability to transiently focus molecules, which can be achieved by both the aster-forming polar filaments above, or apolar filaments that drive bound molecules by active contractile stresses (as described later).

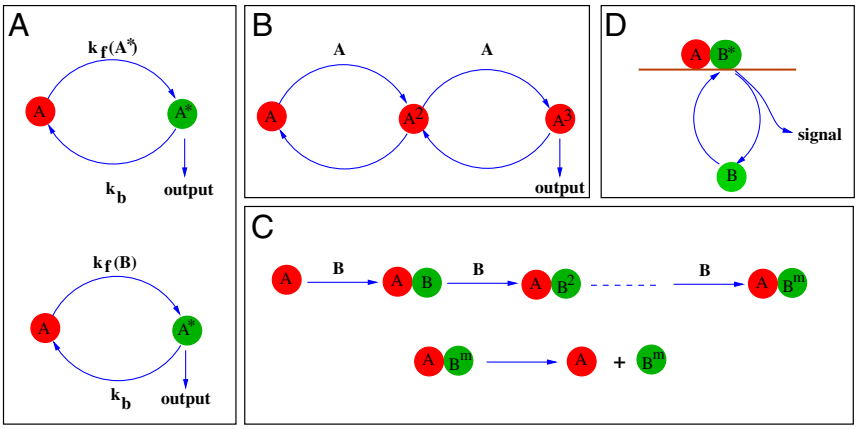

Fig. 2. Generic reaction networks that result in a downstream signal (output). (*A*) $A \rightleftharpoons A^*$, a reaction involving a state change of *A* to its activated homologue A^*. The forward rates can be either allosterically enhanced by the presence of the output $k_f(A^*)$ or modulated by the concentration of an effector molecule or enzyme $k_f(B)$. The reverse rate is k_b. (*B*) $A \rightleftharpoons A^2 \rightleftharpoons \ldots A^n$, where the species A^n alone gives rise to a downstream signal. Such a higher-order reaction acts a *signal integrator*. (*C*) $A + B \rightarrow AB$, where *A* forms a complex with *B*, and $B \rightleftharpoons B^2 \rightleftharpoons \ldots B^m$, where *B* gets cross-linked to each other via a multivalent antibody. Once the cross-linked aggregate reaches a size *m*, it loses its ability to complex with *A*. Such a higher-order reaction leads to *sorting*. (*D*) $B \rightleftharpoons B^*$, $A + B^* \rightleftharpoons AB^*$ the inactive cytoplasmic molecule *B* gets activated to B^*, a membrane bound molecule whose interaction with the cell surface signaling receptor *A* produces a downstream signal. The activation is typically enzymatically catalyzed.

(30) and may be a general mechanism of cellular fine-tuning to obtain optimal efficiency in chemical reactions. Further, for fixed τ_a, the gain shows a sharp transition to $G_\tau < 1$ for larger values of τ_v (Fig. 3*B*); active remodeling can lead to *anticlustering* when the advection velocities are low compared to remodeling rates (13).

These two features are highlighted in a phase diagram (Fig. 3*C*) in the $\tau_a - \tau_v$ plane.

Note that had we taken the active diffusion coefficient of bound particles in the region between asters to be larger than the thermal diffusion coefficient of the unbound particles (31), or if we had increased the aster density ρ_a, then the enhancement in the gain would be much more significant. As we show in ref. 13, the molecules once bound to the filaments are rapidly *funneled* into the cores of the asters.

We extend the above analysis to include a finite backward reaction rate, $k_b > 0$, allowing for spontaneous reversible conformation changes, $A^* \rightarrow A$, a requirement when the reaction dynamics obeys detailed balance. This is relevant to the dynamics of conformational changes of cell surface receptors induced by cooperative ligand binding. An immediate consequence of such spontaneous reversibility is that the saturation output $M_\infty < 1$, for both free diffusion and active dynamics. We therefore define two gains in the active dynamics compared to free diffusion—(*i*) G_τ (gain in activation rate) and (*ii*) $G_M = M_\infty^{\text{act}}/M_\infty^{\text{diff}}$ (gain in saturation output). The qualitative features of G_τ are the same as in the irreversible case.

A qualitative new feature in the analysis of reversible reactions shows up in the behavior of G_M (Fig. 3*D*), where the backward reaction brings in another time scale k_b^{-1}, whose intervention produces the two branches, characterized by $G_M > 1$ at low values of τ_v, and $G_M < 1$ at large τ_v. This provides a unique mechanism for *switching* by modulating the local activity of CA, either via alterations in *K* or by affecting the binding affinities or processivity of myosin motors.

Higher-Order Reactions: Integration, Resetting and Sorting. The enhancement of reaction rates will be much more significant for higher-order reactions involving multimolecular collisions, Fig. 2 *B* and *C*. For diffusion limited processes, the probability of *n*-particle coincidences needed to facilitate higher-order chemi-

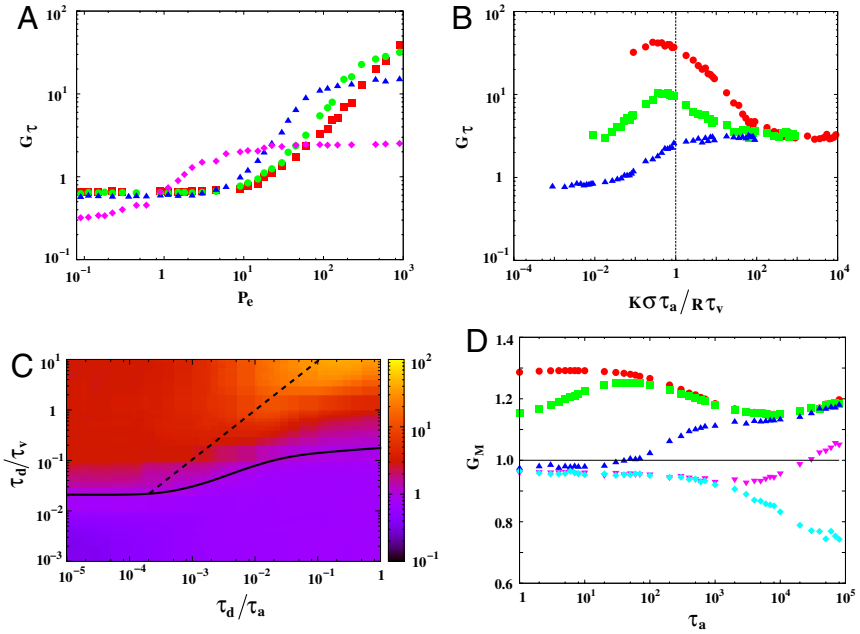

Fig. 3. Irreversible reaction kinetics. (*A*) Gain G_τ versus Peclet number P_e for $\tau_a = 1$ (red square), 10 (green circle), 10^2 (blue triangle), 10^5 (pink diamond). Note the change in the trends for smaller τ_a due to anticlustering. The saturation value increases as τ_a increases from 1 to 10. (*B*) G_τ as a function of active remodeling time for $\tau_v = 0.1$ (red circle), 1 (green square), 10 (blue triangle). (*C*) Phase diagram in τ_d/τ_v versus τ_d/τ_a, both evaluated over the aster size *R*, where the color bar indicates the value of the gain G_τ. The "phase boundary" $G_\tau = 1$ (thick black line) separates the region of high gain from low. The dashed line is the mean field estimate, $K\sigma\tau_a/\tau_v R = 1$, of the active resonance line where G_τ is a maxima. The lower right corner, where $G_\tau < 1$ when τ_a is small, represents the anticlustering phase. (*D*) Reversible reaction kinetics. Gain G_M versus active remodeling time τ_a, for $\tau_v = 0.1$ (red circle), 1 (green square), 10 (blue upper triangle), 10^2 (pink lower triangle), 10^3 (cyan diamond), with $K = 0.9$, shows appearance of two branches at high and low advection velocities, suggesting the possibility of switching as a function of myosin processivity.

cal reactions scales as $c^n \ll 1$, where c is the local concentration. The creation and remodeling of asters can enhance multiparticle encounters, by entrapping a few molecules that seed the further growth of the cluster. We list some of the consequences of the active remodeling dynamics of CA on cell function involving higher-order chemical reactions :

Integration. If the lifetime of the aster is large, then it would be able to recruit and trap multiple molecular species in the cores of asters. This could lead to signal integration and thresholding, desirable features of a signaling process to convey information downstream in a noisy environment (Fig. 2*B*).

Resetting. After acting as signaling platforms/catalytic centers, the aster breakup dynamics provides a natural mechanism for resetting the system to its presignaling state. This actin-dependent resetting could be relevant for the signaling specificity of the promiscuous Ras-family proteins that make actin-dependent clusters (8). Individual Ras proteins can potentially engage with multiple downstream effectors based on the configuration adopted by the Ras molecule in the cluster (32). Actin-dependent remodeling would provide a mechanism to reset the configuration of Ras to its presignaling state for it to engage anew with another downstream effector.

Sorting. Consider two molecules A and B that cohabit the same cluster, with B capable of binding with high affinity to a multivalent antibody. As an example, we consider the coclustering of two different species of GPI-APs on the cell surface, GFP-GPI and DAF (decay activating factor), where DAF is capable of being cross-linked by an antibody (11). Here we found that although the two GPI-APs cohabit in the same nanocluster, cross-linking one species with an antibody was able to segregate the cross-linked species from the other species. In our model, the high binding affinity aggregation of B can be viewed as a chemical reaction, where the interaction of B with the k-valent antibody produces higher-order aggregates, denoted by $B^2,B^3,\ldots B^k$ (Fig. 2*C*). It is reasonable to expect that the aggregate breaks away from the aster when its size is larger than a threshold $m \leq k$. This could be either because the effective unbinding rate to the cytoskeleton is large or that the underlying aster gets destabilized. This ultimately leads to a sorting out of the cross-linked species, providing a natural explanation of the results of antibody-induced segregation (11).

Aster as an Enzyme with a High Hill Coefficient. When the lifetime of the aster is of the order of the typical reaction time or larger, then the aster can be thought of as an enzyme, catalyzing the chemical reaction. We will call this a quasienzyme, because the aster is a defect configuration of the active filaments with a finite lifetime. The interaction range of this quasienzyme is the aster size R and the interaction strength is related to Kc_0R^2.

As an example we consider the simplest chemical reaction, Fig. 2*A*; denoting the quasienzyme as E, we have,

$$E + A \underset{k_-}{\overset{k_+}{\rightleftharpoons}} EA \overset{k_{\text{cat}}}{\rightarrow} A^* + E \qquad [5]$$

or even $E + A + B \rightleftharpoons EAB \rightarrow A^* + E$. The stochastic breakup and reformation of the quasienzyme does two things—(*i*) the number of enzymes is conserved in the mean and (*ii*) during remodeling events, the aster can be viewed as undergoing long-range uncorrelated hops. The reaction schematized in Eq. **5** can then be analyzed by Michaelis–Menten kinetics—in the limit of large capture cross-section Σ, $k_+ \sim \tau_v^{-1}$ and $k_- \sim \tau_a^{-1} + t_{\text{sw}}^{-1}$, and the product formation rate is given by

$$\frac{d[A^*]}{dt} = \frac{k_{\text{cat}}[E]_{\text{total}}[A]}{[A] + K_M}, \qquad [6]$$

where $K_M = (k_- + k_{\text{cat}})/k_+$ is the usual Michaelis–Mentin constant and increases with increasing aster concentration ρ_a. Note that the reaction rates here are not "hardwired" molecularly, but are regulated by the local actin dynamics. The remodeling dynamics makes the effective concentration of the quasienzyme larger than its bare value, i.e., the difference between the free and total enzyme concentration is negligible. In general, increasing the number of asters increases the probability of capture for advection into the core and hence the collisional probability for enzymatic reaction.

In the limit that $[A] \ll K_M$, the rate of product formation is given by $(k_{\text{cat}}/K_M)[E]_{\text{total}}[A]$. For kinetically perfect enzymes, this rate is determined by the collisional probability between enzyme and substrate. For inert molecules, this is given by the diffusion rate τ_d^{-1} over the scale of the aster R, whereas for passive molecules this is given by τ_v^{-1}. Again, for a high Peclet number we obtain a significant gain in reaction rate due to the advection into asters.

However, the real import of such an active recruitment mechanism is as natural facilitators of reaction cascades such as

$$E + A \rightleftharpoons E_1 \rightarrow E + A^* \qquad E_1 + A \rightleftharpoons E_2 \rightarrow E_1 + A^* \ldots,$$

where the resulting cooperativity could result in a high Hill coefficient and consequent switch-like behavior desirable in many signaling processes.

Discussion

In this paper we have proposed a mechanism whereby a living cell can spatiotemporally regulate and enhance chemical reactions by locally modulating the active remodeling dynamics of the cytoskeleton and its binding to molecules involved in the reaction. Even though our detailed quantitative analysis has been carried out in the context of chemical reactions where the reactants are advected by polar active filaments on the cell surface, the qualitative results should be valid in a more general setting within the cell. Indeed, the most relevant feature of the active cytoskeletal dynamics that we exploit is the ability to transiently focus molecules. This can be achieved by polar filaments forming asters that drive bound molecules by active advection (Fig. 1) or apolar filaments that drive bound molecules by active contractile stresses (Fig. 4). As mentioned in *Model*, the filament current generated by active stresses is given by $\mathbf{J} = -Wc\nabla \cdot cQ \approx -W\nabla c + \ldots$ (16). For contractile stresses, $W < 0$ (16), resulting in a *negative* diffusion-like term that brings molecules together (Fig. 4).

We highlight the unique concepts that emerge from our study of chemical reactions in the living state. For instance, we have defined an *active Peclet number* as a useful measure of the relative contribution of active advection to chemical reaction rates. We have introduced the concept of *active resonance*, arising as a consequence of the competition between active advection and active remodeling of the contractile elements, at which the gain in the rates of chemical reactions is maximal. This suggests that the cell can locally fine-tune the activity so as to meet the resonance condition. The competition between remodeling of and advection along active filaments can even lead to local *anticlustering* of molecules; this and the *active switching* discussed in the context of reversible chemical reactions can contribute to local regulation of chemical reactions. These ideas will have an impact on our understanding of the spatial control of signaling reactions and their dynamics (33).

The spatial organization of active contractile elements on the cell surface or in the interior of the cell could have implications in the conformational spread by allosteric modification of receptor proteins—in the context of chemotactic receptors on the bacterial cell surface, it has been suggested that receptors organize in a fixed two-dimensional lattice in order for conformation changes

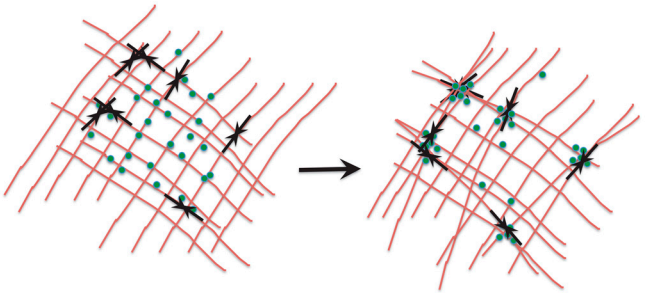

Fig. 4. The schematic shows how transient focusing of bound molecules can be achieved by an apolar filament mesh. Myosin motors (inward double arrows) bound to actin filaments (lines) apply active contractile stresses upon activation, which locally compress the mesh. Reactant molecules (dots) bound to the meshwork will be brought together for chemical reaction by such local contractile stresses. The mesh can locally remodel due to myosin turnover.

to propagate over large distances (34). Here we propose that in certain situations, cell surface receptors can be actively organized into the cores of asters forming a dynamic pattern, whose lifetime can be regulated by the remodeling dynamics of the CA. Evidence for this comes from recent experiments in our laboratory, where adding an actin-binding domain to a transmembrane protein confers an ability to be patterned by the underlying cortical actin dynamics, similar to that observed for GPI-anchored proteins (13). These results suggest that the capacity to engage with the dynamic actin cytoskeleton may be available for any protein that has actin-binding domains or has protein-interacting domains such as the PDZ domains that may confer CA-binding capacity (35). These properties will hugely enhance the scope and influence on CA on the dynamics of signaling conceived as a series of assembly reactions.

In the context of the cell surface, our proposal has a direct bearing on molecules, such as lipid-tethered GPI-APs and Ras signaling molecules, which constitutively form transient nanoclusters regulated by the active remodeling of the underlying CA (11, 13, 36). The sorting and segregation of GPI-anchored proteins nanoclusters from proteins cross-linked by antibodies (11) are also easily explained by a continuous and active remodeling mechanism.

Our study is of relevance to the actin-dependent clustering of activated T-cell receptors (TCRs) with their coreceptors and regulators (37, 38), where TCRs first form actin-sensitive microclusters (39) and these then are driven toward the cores of micron-scale bulls-eye patterns. In the context of nuclear signaling, we propose that transcription reactions at target gene foci are spatiotemporally regulated by active stresses generated by ATP-dependent chromatin remodeling proteins. Consistent with this idea, there is recent evidence for ATP-dependent directed movement of transcription factories towards gene loci (5).

We believe that the kinetic regulation of chemical reactions that takes place in the living cell will involve distinctly unique concepts, some of which are elucidated here. We look forward to experimental investigations of the proposed active cytoskeletal-based enhancement of chemical reactions in both carefully reconstituted cell systems and in vivo.

ACKNOWLEDGMENTS. A.C. and M.R. thank Indo French Centre for the Promotion of Advanced Research Project 3504-2, and S.M. and M.R. thank Human Frontier Science Program for grants. S.M. acknowledges a J. C. Bose Fellowship from the Department of Science and Technology (India). The authors are pleased to acknowledge that part of this research was performed while in residence at the Kavli Institute for Theoretical Physics and was supported in part by the National Science Foundation under Grant PHY05-51164.

1. Monod J, Wyman J, Changeux JP (1965) On the nature of allosteric transition: A plausible model. *J Mol Biol* 12:88–118.
2. Yu EW, Koshland DE (2001) Propagating conformational changes over long (and short) distances in proteins. *Proc Natl Acad Sci USA* 98:9517–9520.
3. Bray D, Levin MD, Morton-Firth CJ (1998) Receptor clustering as a cellular mechanism to control sensitivity. *Nature* 393:85–88.
4. Zerial M, McBride H (2001) Rab proteins as membrane organizers. *Nat Rev Mol Cell Biol* 2:107–117.
5. Sinha DK, Banerjee B, Maharana S, Shivashankar GV (2008) Probing the dynamic organization of transcription compartments and gene loci within the nucleus of living cells. *Biophys J* 95:5432–5438.
6. Suzuki KGN, et al. (2007) GPI-anchored receptor clusters transiently recruit Lyn and G alpha for temporary cluster immobilization and Lyn activation: Single-molecule study. *J Cell Biol* 177:717–730.
7. Hancock J (2003) Ras proteins: Different signals from different locations. *Nat Rev Mol Cell Biol* 4:373–384.
8. Plowman S, Muncke C, Parton R, Hancock J (2005) H-ras, K-ras, and inner plasma membrane raft proteins operate in naoclusters with differential dependence on the actin cytoskeleton. *Proc Natl Acad Sci USA* 102:15500–15505.
9. Gureasko J, et al. (2008) Membrane dependent signal integration by the Ras activator Son of sevenless. *Nat Struct Mol Biol* 15:452–461.
10. Goswami D, et al. (2008) Nanoclusters of GPI-anchored proteins are formed by cortical actin-driven activity. *Cell* 135:1085–1097.
11. Sharma P, et al. (2004) Nanoscale organization of multiple GPI-anchored proteins in living cell membranes. *Cell* 116:577–589.
12. van Zanten TS, et al. (2009) Hotspots of GPI-anchored proteins and integrin nanoclusters function as nucleation sites for cell adhesion. *Proc Natl Acad Sci USA* 106:18557–18562.
13. Gowrishankar K (2009) Dynamics of shape and composition of an active composite membrane. PhD thesis (Raman Research Institute, Bangalore, India).
14. Toner J, Tu Y (1995) Long-range order in a two dimensional dynamical XY model: How birds fly together. *Phys Rev Lett* 75:4326–4329.
15. Simha RA, Ramaswamy S (2002) Hydrodynamic fluctuation and instabilities in ordered suspensions of self-propelled particles. *Phys Rev Lett* 89:058101.
16. Hatwalne Y, Ramaswamy S, Rao M, Simha RA (2004) Rheology of active-particle suspensions. *Phys Rev Lett* 92:118101.
17. Liverpool TB, Marchetti MC (2003) Instabilities of isotropic solutions of active polar filaments. *Phys Rev Lett* 90:138102.
18. Kruse K, Joanny JF, Julicher F, Prost J, Sekimoto K (2004) Asters, vortices, and rotating spirals in active gels of polar filaments. *Phys Rev Lett* 92:078101.
19. Kruse K, Joanny JF, Julicher F, Prost J (2005) Generic theory of active polar gels: A paradigm for cytoskeletal dynamics. *Eur Phys J E Soft Matter* 16:5–16.
20. Salbreux G, Prost J, Joanny JF (2009) Hydrodynamics of cellular cortical flows and formation of contractile rings. *Phys Rev Lett* 103:058102.
21. Howard J, Grill SW, Bois J (2011) Turing's next steps: The mechanochemical basis of morphogenesis. *Nat Rev Mol Cell Biol* 12:400–406.
22. Rajaraman R (1987) *Solitons and Instantons* (North-Holland, Amsterdam).
23. Fehon GR, McClatchey AI, Bretscher A (2010) Organizing the cell cortex: The role of ERM proteins. *Nat Rev Mol Cell Biol* 11:276–287.
24. Gimona M, Djinovic-Carugo K, Kranewitter WJ, Winder SJ (2002) Functional plasticity of CH domains. *FEBS Lett* 513:98–106.
25. Kampen V (2004) *Stochastic Processes in Physics and Chemistry* (North-Holland, Amsterdam).
26. Loverdo C, Bénichou O, Moreau M, Voituriez R (2008) Enhanced reaction kinetics in biological cells. *Nature Phys* 4:134–137.
27. Allen MP, Tildesley DJ (1987) *Computer Simulation of Liquids* (Oxford Univ Press, Oxford, UK).
28. Bray D (2001) *Cell Movements: From Molecules to Motility* (Taylor and Francis, New York).
29. Guyon E, Hulin JP, Petit L, Mitescu CD (2001) *Physical Hydrodynamics* (Oxford Univ Press, Oxford, UK).
30. Gammaitoni L, Hänggi P, Jung P, Marchesoni F (1998) Stochastic resonance. *Rev Mod Phys* 70:223–287.
31. Brangwynne CP, Koenderink GH, MacKintosh FC, Weitz DA (2008) Cytoplasmic diffusion: Molecular motors mix it up. *J Cell Biol* 183:583–587.
32. Abankwa D, Gorfe AA, Inder K, Hancock JF (2010) Ras membrane orientation and nanodomain localization generate isoform diversity. *Proc Natl Acad Sci USA* 107:1130–1135.
33. Groves JT, Kuriyan J (2010) Molecular mechanisms in signal transduction at the membrane. *Nat Struct Mol Biol* 17:659–665.
34. Bray D, Duke T (2004) Conformational spread: The propagation of allosteric states in large multiprotein complexes. *Annu Rev Biophys Biomol Struct* 33:53–73.
35. Fehon GR, McClatchey AI, Bretscher A (2010) Organizing the cell cortex: The role of ERM proteins. *Nat Rev Mol Cell Biol* 11:276–287.
36. Mayor S, Rao M (2004) Rafts: Scale-dependent, active lipid organization at the cell surface. *Traffic* 5:231–240.
37. Grakoui A, et al. (1999) The immunological synapse: A molecular machine controlling T cell activation. *Science* 285:221–227.
38. Kaizuka Y, Douglass AD, Varma R, Dustin ML, Vale RD (2007) Mechanisms for segregating T cell receptor and adhesion molecules during immunological synapse formationin Jurkat T cells. *Proc Natl Acad Sci USA* 104:20296–20301.
39. Varma R, Campi G, Yokosuka T, Saito T, Dustin ML (2006) T cell receptor-proximal signals are sustained in peripheral microclusters and terminated in the central supramolecular activation cluster. *Immunity* 25:117–127.